Eur. Phys. J. B **15**, 557–566 (2000)

THE EUROPEAN PHYSICAL JOURNAL B

EDP Sciences

Scaling approach of the convective drying of a porous medium

P. Coussot[a]

LMSGC[b], 2 allée Kepler, 77420 Champs-sur-Marne, France

Received 7 June 1999 and Received in final form 25 October 1999

Abstract. We propose a simplified, theoretical approach of the evolution of liquid distribution during the convective drying of a granular packing. In the absence of gravity effects three regimes are distinguished according to the relative importance of surface evaporation, capillarity or evaporation from the interior of the sample. The evolution of the drying rate as a function of the saturation can be inferred from the characteristic velocities associated to each of these effects. We also carried out drying experiments of bead packings saturated with ethanol, at four different velocities of the boundary convection current, and with bead size ranging from 4.5 to 100 μm. The drying curves exhibit different regimes with a scaling as a function of particle radius and current velocity as predicted by the theory.

PACS. 68.10.-m Fluid surfaces and fluid fluid interfaces – 81.05.Rm Porous materials; granular materials – 92.40.Je Evaporation

1 Introduction

Porous materials in contact with the atmosphere such as rocks, soils, bricks, concrete, cement, wood or roads are constantly submitted to imbibition-drying cycles which critically influence their properties and their life. For these materials the slow drying at ambient temperature under the action of a convection current along a free surface is a very common process. The drying of porous media, which is also of great interest in industrial processes, has been extensively modelled within the framework of thermodynamics [1]. In that case it is necessary to take into account temperature and pressure gradients within the material [2,3]. From current models it is nevertheless hard to distinguish the dominant mechanisms in process. Here we propose a straightforward approach of the drying of a model porous medium (a granular packing) based on global, though approximate, physical arguments (pore structure and characteristic velocities) which make it possible to simply predict the features of drying over a wide range of conditions.

We consider the drying, at ambient temperature (T), of a liquid initially saturating a random packing of rigid spheres (of characteristic radius R) in a cylindrical vessel of cross-section S and height H_0, as a result of gas convection along its upper, horizontal, free surface (see Fig. 1). The other boundaries of the bead pack are in contact with approximately isothermal, rigid, impermeable, surfaces. The temperature of the convected gas remains close to the ambient temperature so that temperature gradients remain weak during the experiment. Adsorption of liquid on particle surface is neglected and the solid particles are non-hygroscopic. Under these conditions drying fundamentally consists in replacing liquid by air within a fixed solid volume with possible liquid counterflows at slow evaporation rates [4]. We shall only deal with sufficiently slow processes that can be considered at each time as in pseudo steady-state regime.

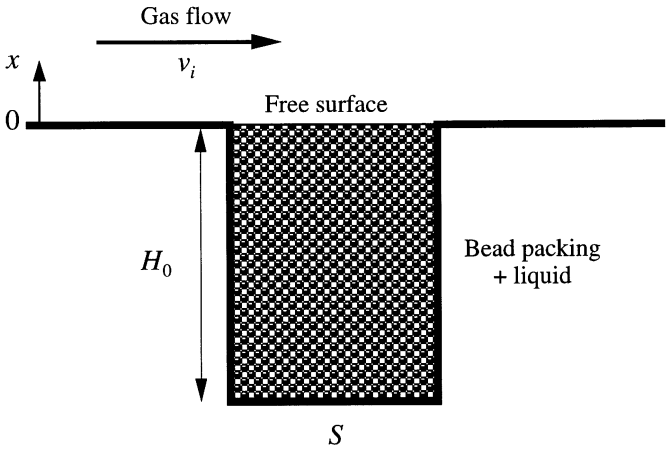

Fig. 1. Principle of the convective drying of a porous medium.

In practice the drying curve, *i.e.* the drying rate (see Sect. 2) as a function of liquid content, of such a material has been separated into three periods to which physical processes have been tentatively associated [3,5–9]: 1) a period of constant-rate (CR) of drying (also called funicular regime because the liquid is supposed to be mobile), generally associated with the existence of a continuous liquid network throughout the sample; 2) a first

[a] e-mail: philippe.coussot@lcpc.fr
[b] UMR 113 LCPC-CNRS

decreasing-rate period (FDR) during which the liquid close to the surface clearly breaks into discontinuous wet patches and the surface temperature slightly increases; 3) a second decreasing-rate (SDR) period, generally associated with a discontinuous liquid network within the porous medium (pendular regime) and the development of a dry receding front from the free surface of the sample. The rate of drying in the three different periods has mainly been modelled numerically from a set of equations taking into account vapour and liquid transfers along with boundary conditions. In general the predictions of these models, which often rely on the use of more or less adjustable parameters (vapour diffusion coefficient and liquid permeability) and some simplifying hypotheses concerning the physical processes, are in reasonable agreement with experimental results essentially during the first stages of drying. However the possibility of making accurate predictions appears doubtful not only because of the limitations of the theory but also because of the inaccuracies of experimental results [10,11]. In particular the critical time at which the FDR period starts has generally been correctly predicted by these models but not the drying rate beyond this time [6].

Physical approaches of drying intended to identify drying regimes and to determine drying rate as a function of material characteristics surprisingly lack. In this domain the deepest insight has been provided by Van Brakel [12] on the basis of an extensive review of existing experimental results and physical analyses. In particular this author showed that: the drying rate during the (CR) period is in fact not exactly constant; it is highly doubtful that a liquid film is always present at the sample surface during this period; a (CR) period does not occur if the capillary liquid transport cannot sustain the rate of evaporation.

Apart from these basic, physical considerations, some authors [4,13–15] studied the characteristics of dry fronts propagating in porous media with the help of invasion percolation principles. The fundamental assumption of these works is that as drying proceeds a dry region progressively extends from the free surface towards the interior of the porous medium. Under these conditions this is a situation of slow drainage for which capillary effects play a major role so that the air penetration through the sample can basically be described by invasion percolation concepts. However the field of application of these models remains questionable since most measurements of water content distribution within slowly drying porous media show that a dry region develops only during the ultimate stage of drying [12,16]. In the absence of gravity effects only one experimental work [4] seems to support the assumption of a dry front propagating from sample free surface. It relies on lateral observations of an opaque region progressing through a refractive-index-matched water-silica spheres mixture. We emphasize that this opacity simply proves the existence of some water-air interfaces but cannot be associated to an air content. Finally, in agreement with our own lateral observations of drying of water-bead packings, we believe that Shaw's observations correspond to the preliminary stages of drying when the water-air interface initially penetrates each REV of the medium, the saturation remaining close to its maximum. In the following we shall neglect this period which is in general a short transient regime.

The present work relies on the idea that dominant mechanisms can be associated to the different drying regimes from which drying rate expressions in each regime can be deduced. In this way we need to associate some, necessarily approximate, characteristic velocities to the main processes of liquid or vapor motion through the porous medium. A comparison of these velocities will make it possible to distinguish the dominant mechanisms at the different stages of drying.

2 General expression for the drying rate

In the following the description of physical phenomena within the porous medium must be understood as averaged over a sample volume sufficiently large compared to its heterogenities, *i.e.* an elementary representative volume (REV) [1]. In addition the sample is assumed to be sufficiently wide for edge effects to be negligible. Thus the physical phenomena are independent on the position in any plane parallel to the free surface and, by symmetry, the average (over an REV) motion of liquid or vapor is parallel to the direction x perpendicular to this surface (we take the origin $x = 0$ at the free surface and $x > 0$ out of the sample).

Basically the liquid escapes from the sample (in the form of vapor) by going through its free surface as a result of evaporation. The drying rate (V_{d}) is defined as the rate at which this vapor escapes from the sample by unit surface:

$$V_{\mathrm{d}} = \frac{1}{S}\frac{\mathrm{d}M}{\mathrm{d}t}\cdot \tag{1}$$

Since within the sample this vapor is in the form of vapor or liquid we have:

$$M = \rho\Omega_{\mathrm{L}} + \bar{n}\Omega_{\mathrm{v}}. \tag{2}$$

In this equation, Ω_{L} and Ω_{V} are respectively the liquid and vapour volumes, ρ is the liquid density (considered uniform and constant) and $\bar{n}$ the mean vapor density defined as:

$$\bar{n} = \frac{1}{\Omega_{\mathrm{V}}}\int_{\Omega_{\mathrm{V}}} n\mathrm{d}\Omega \tag{3}$$

where n is the local (over an REV) vapour density (the mass of vapour by unit volume ($n \ll \rho$)). We can prove that $\bar{n}$ is almost constant for some regimes by anticipating on our further description of drying regimes. Indeed for a regime in which the liquid is dispersed within all the granular packing (evaporative and capillary regimes) n remains equal to the saturation vapour density except in a few layers close to the free surface. In addition it may be shown that this is still true when a significant region of the porous medium is dry ("receding regime"), using in

particular the linear profile of vapour density within the dry region, except when the saturation reaches values of the order of n/ρ. Using now the conservation of the total volume available for gas or liquid ($\Omega_{\rm L} + \Omega_{\rm V} = {\rm Cst.} = \Omega_0$ where Ω_0 is the total volume available for liquid or vapour) we finally obtain from (1) and (2):

$$V_{\rm d} = -\frac{1}{S}(\rho - \bar{n})\frac{{\rm d}\Omega_{\rm L}}{{\rm d}t} \approx -\frac{1}{S}\rho\frac{{\rm d}\Omega_{\rm L}}{{\rm d}t}\,. \tag{4}$$

Thus the drying rate is simply the rate at which the liquid disappears from the sample. Moreover, using the saturation ϕ, *i.e.* the ratio of the effective liquid volume to the total volume available for liquid within the granular pack, we have:

$$\Omega_{\rm L} = \omega S\int_0^{H_0}\phi(x){\rm d}x = \Omega_0\bar{\phi} \tag{5}$$

where ω is the porosity and $\bar{\phi}$ the mean saturation (over the sample). Finally the drying rate is given by:

$$V_{\rm d} = -\frac{M_0}{S}\frac{{\rm d}(\bar{\phi})}{{\rm d}t} \tag{6}$$

where M_0 is the initial mass of liquid in the saturated material. This means that if in addition we can express the drying rate as a function of boundary conditions and material properties we shall obtain from (6) an equation giving the saturation as a function of time. Our approach in terms of regimes will effectively make it possible to express $V_{\rm d}$ as a function of boundary conditions and saturation only.

Note that the pseudo steady-state hypothesis means that during each elementary step of the drying process the instantaneous drying rate can be computed by assuming that the liquid and vapour distributions do not change significantly during this step. More precisely this requires that for an elementary measured variation $\Delta\bar{\phi}$ the corresponding variation in velocity must be much smaller than the mean velocity during this period: $\Delta V_{\rm d} \ll V_{\rm d}$.

3 Rate of evaporation

The rate of evaporation ($V_{\rm e}$) from a liquid surface depends on the diffusion of vapor through air whose rate is proportional to the gradient of vapor density:

$$V_{\rm e} = -D\frac{{\rm d}n}{{\rm d}x} \tag{7}$$

where D is the coefficient of diffusion of the vapour in the gas. Remark that n is proportional to the pressure and inversely proportional to the temperature, while D is proportional to the square root of the temperature. Two asymptotic situations can now be considered. If the interface is at a distance H much larger than the mean free path (λ) of vapour molecules from a surface along which the vapour density is fixed to a small value n_0, and if there is no gas flow between the two surfaces, the conservation of vapour mass in steady state implies that ${\rm d}n/{\rm d}x$ is constant. Under these conditions we obtain the following simple expression for the rate of evaporation:

$$V_{\rm e} = D\frac{(n_{\rm v} - n_0)}{H} = \frac{K}{H} \tag{8}$$

where $n_{\rm v}$ is the saturation vapour density and K a function of the temperature and pressure. When the interface is in direct contact with a convection current the variation of ${\rm d}n/{\rm d}x$ with x depends on the gas velocity profile [17, 18]. Since gas flows are generally in a turbulent regime the velocity significantly varies only over a short distance (the boundary layer) from the interface. Within this framework a rough approximation [19] consists in considering that ${\rm d}n/{\rm d}x$ is constant in a region of thickness δ of the order of this boundary layer while the vapour density (n_0) is maintained constant in the region of nearly uniform velocity. In that case we obtain the following estimate for the rate of evaporation:

$$V_{\rm e} = D\frac{(n_{\rm v} - n_0)}{\delta} = \frac{K}{\delta}\,. \tag{9}$$

Note that this approximation at least makes it possible to reproduce the tendency of the rate of evaporation to increase with gas velocity, since the boundary layer is a decreasing function of velocity.

Let us now consider the evaporation from a porous material. When the free surface of the sample is covered by a liquid film exposed to the convection current the rate of evaporation is given by (9). If only some wet patches are exposed to the convection current (possibly perturbed by the roughness (of the order of the size of particles) of the free surface of the sample), the rate of evaporation is lower but has in general the same order of magnitude except when the surface fraction occupied by the wet patches is too small (say below 0.1 according to the results of Suzuki and Maeda [17]). The rate of evaporation under these conditions will be referred to as $V_{\rm e}$.

When the first liquid volumes are at a distance H (this will be referred to as the liquid-limit) larger than few particle diameters from the free surface, evaporation now occurs in the form of simple diffusion between $-H$ and 0 and diffusion through the convection current beyond 0. Remark that at a relatively short distance below the liquid-limit a liquid patch is surrounded by other small liquid patches. The mass conservation for the vapour density in pseudo steady-state ($\boldsymbol{\nabla}\cdot\mathbf{V}_{\rm e} = 0$) under such boundary conditions implies that n remains very close to $n_{\rm v}$ in the corresponding gas volume so that evaporation is negligible from the corresponding patches. As a consequence only a small layer of the porous material below the liquid-limit will provide almost all the diffusing vapour. On the basis of the results of Suzuki and Maeda for the evaporation from the free surface of a porous medium we can consider that the evaporation rate from this layer is given by an equation similar to (8) with now a coefficient of diffusion (D^*) depending on the surface fraction of patches, *i.e.* on the saturation, and on the tortuosity of the porous structure (θ). Since pressure and temperature only affect the kinetic properties of the molecules while the liquid

fraction and tortuosity are purely geometrical characteristics it is natural to assume that, as long as the mean free path of molecules remains much smaller than the characteristic pore size, D^* is simply obtained by multiplying D by a factor $f(\theta,\phi) < 1$. Finally the rate of evaporation in steady state is now given by (8) and (9) in which the vapour density at the boundaries takes the following values: $n(-H) = n_{\rm v}$; $n(0) = n_{\rm i}$; $n(\delta) = n_0$. Eliminating $n_{\rm i}$ from these equations gives:

$$V_{\rm e}^* = \frac{f}{1 + f\delta/H}\frac{K}{H}\,. \tag{10}$$

As soon as H is much larger than δ we simply have $V_{\rm e}^* = fK/H$. In addition the continuity between the two evaporating processes is ensured by the fact that $V_{\rm e}^*(h) \to V_{\rm e}$ when $H \to 0$.

4 Capillary transfers

During slow drying liquid motions are fundamentally caused by differences in capillary pressure between two points of the liquid network. Since complex motions of liquid within the granular packing are involved, in particular counterflows (see [4] and Sect. 5.1), it is rather hard to precisely compute the characteristic velocity associated to this phenomenon. Considering that it globally leads to a liquid motion through the grain network towards the sample free surface we suggest to estimate this velocity by assuming that it is a liquid motion through the porous network caused by a difference in capillary pressure between the top and the bottom of the sample.

Now the rate of liquid flow under the action of capillarity depends on the liquid distribution within the granular network but it is also a rather difficult problem to determine this distribution since it depends on the pore structure and on the interfacial tensions between the liquid and the gas, the liquid and the solid, and the solid and the gas. We shall neglect the effect of particle roughness, which at least means that this roughness is much smaller than particle radius. Here we shall simply consider that, during the drainage induced by drying, for a given value of saturation, the liquid distribution in the granular packing is given. Since this liquid distribution is entirely determined by the particle configuration and by capillary effects which vary proportionally to the pore size, it is a function of ϕ, ω and R only. This means that the liquid network has a permeability (k) which depends on the same parameters. On the basis of various theoretical and experimental results we can write:

$$k = F(\phi,\omega)R^2 \tag{11}$$

where F is an increasing function of ϕ and a decreasing function of ω. If we assume that this function can be written in the form $F = f_0(\omega)f_1(\phi)$ its value might for example be estimated from the theoretical Koseny-Carman formula for the permeability of the saturated medium $f_0(\omega) = (1-\omega)^3/45\omega^2$ and from the usual empirical expression [22] for the permeability of an unsaturated porous medium: $f_1(\phi) = (\phi-\phi_{\rm c})^3/(1-\phi_{\rm c})^3$ where $\phi_{\rm c}$ is a critical saturation below which the liquid network is discontinuous ($f_1(\phi < \phi_{\rm c}) = 0$).

The motion of liquid through the solid network under a gradient of pressure (p) is correctly described by the Darcy's law:

$$\frac{{\rm d}p}{{\rm d}x} = \frac{\mu V}{k} \tag{12}$$

where μ is the liquid viscosity and V the resulting mean velocity. During drying, in the absence of gravity effects, no pressure gradient is applied by external means to the liquid network. Only some heterogeneity in capillary pressure throughout the sample can cause a liquid motion. There are various types of such heterogeneities and we shall retain only one which corresponds to a critical situation. Consider a material in which the saturation is uniform. If the evaporation is extremely rapid the liquid-gas interface retreats within the granular packing while the saturation below this interface does not vary. During such a phenomenon the liquid tends in particular to disappear from around the points of contact between particles where the thickness of the liquid films takes its minimum value. Thus the mean curvature of the interface (in an REV) is at its minimum and the capillary pressure is at its maximum ($p_{\rm c}$). Using now scaling arguments similar to those used above for the liquid distribution under capillary effects only, we deduce:

$$p_{\rm c} = \frac{\alpha}{R} \tag{13}$$

where α is a function of the three interfacial tensions above mentioned. The pressure (and thus the liquid velocity) at a given distance from the liquid-limit satisfies a differential equation obtained by introducing the expression for the velocity from the Darcy's law into the mass conservation. In order to directly obtain an approximate expression for the characteristic velocity resulting from this liquid distribution we shall simply assume that at the maximum distance H_0 from the liquid-limit and within the wet region the capillary pressure is equal to $p(\bar{\phi})$, *i.e.* the capillary pressure resulting from the liquid distribution for the mean saturation in equilibrium in the porous structure. In addition we assume that the velocity can be deduced with the help of the Darcy's law in which a constant permeability $k(\bar{\phi})$ is used. The pressure gradient thus writes $(\alpha/R - p(\bar{\phi}))/H_0$ and the corresponding critical liquid velocity is given by:

$$V_{\rm c} = \frac{k(\bar{\phi})}{\mu H_0}\left(\frac{\alpha}{R} - p(\bar{\phi})\right). \tag{14}$$

In general $p(\bar{\phi})$ is much smaller than α/R so that we have:

$$V_{\rm c} \approx \frac{\alpha F(\bar{\phi})R}{\mu H_0}\,. \tag{15}$$

Obviously this value is a rough approximation of the liquid velocity under capillary effects under the conditions described in Section 5.1. Indeed we shall see that the exact process is a progressive replacement of liquid by gas, by fits and starts and even some significant rebalancing over the sample but we emphasize that (15) probably contains the basic, scaling dependency on the variables of the problem.

At last note that the pressure loss by unit length due to gravity is equal to ρg so that gravity is negligible compared to capillary effects when:

$$\frac{\rho g R H_0}{\alpha} \ll 1 \tag{16}$$

in which in most cases $\alpha = \beta\sigma$ where σ is the liquid-gas interfacial tension and β a coefficient of the order of the ratio of the particle radius to some characteristic size of the pores (for usual systems β can reasonably be taken to 5).

5 Drying regimes

5.1 The evaporative regime: $V_e \ll V_c$

As some liquid is withdrawn because of evaporation from the top of the sample, the curvature of the liquid-gas interface decreases so that the capillary pressure increases. Ultimately it should even reach its critical value. However this does not occur in this regime since for a much lower capillary pressure the characteristic liquid velocity under the action of the corresponding pressure gradient is as large as the evaporation rate. When this occurs the flow of liquid towards the free surface of the sample balances the evaporation and the limit between the wet and the dry region, which will now be referred to as the liquid-limit, (almost) no longer moves towards the interior of the porous medium.

In fact, in this regime, at each step of the process as long as the liquid network is continuous, capillary effects have time to balance, *i.e.* the (mean) curvature of the gas-liquid interfaces is uniform in the sample. Due to the evaporation along the free surface the liquid-gas interface withdraws and reaches the first particle layer. Then, since the liquid cannot withdraw from around the points of contact between particles, fingers tend to penetrate the packing where the curvature is the largest. At this stage this is nothing more than an invasion percolation process. However a peculiar effect can soon occur. If any gas finger reaches a region where its curvature can be larger it suddenly invades this region while the liquid at the same time more or less completely fills in the tail of this finger or of other fingers. This effect can be better understood with the help of an ideal porous model as proposed in Figure 2. Subsequently the original gas-fingers form again, reach the region of largest curvature which is now filled with gas and the progression can go on under the same principles. This effect is probably at the origin of the peculiar density profiles during drying of a bead packing made of two layers of beads of different diameters: the layer with the largest particles close to the bottom first empties almost completely before the upper layer starts emptying [5,12,20,21]. As already suggested by Shaw [4] this in fact means that this process does not completely follow the rules of the invasion percolation process. The fundamental difference is that in drying the external pressure which conditions the advance of the gas does not vary monotonously. As a consequence, for a granular packing made of two layers as described above, as soon as one of the fingers formed in the upper layer has reached the bottom layer this layer is rapidly invaded by gas while the upper region can be filled back.

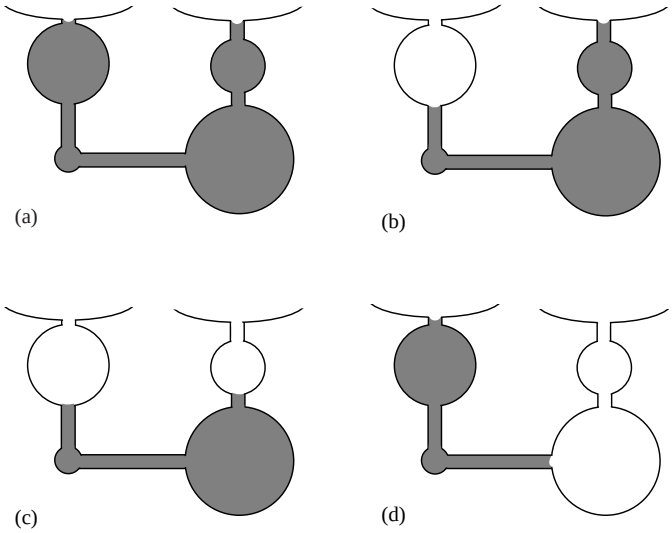

Fig. 2. Scheme of principle of the equilibration process within the liquid network. We consider the evaporation of a liquid situated in a series of basins of various sizes connected by channels of identical size. The basins are initially full of liquid (a) then the largest basin along the liquid-gas interface is filled with gas (b). Afterwards the next largest basin is filled up (c). The peculiar effect occurs when the next largest basin being larger than one of the basin just filled, the former is filled while the latter is emptied (d).

Apart from the preliminary stage during which the liquid-gas interface initially penetrate the whole medium (see Sect. 1), the saturation in the evaporative regime remains uniform except in a very small region close to the free surface where it is almost equal to zero. As the saturation decreases the shape of the liquid-gas interface along the liquid-limit changes but the liquid-limit remains almost fixed. Finally the drying rate remains equal to the evaporation rate V_e from the free surface of the sample, modulated by the progressive, slight intrusion of the interface inside the granular packing (*cf.* Fig. 3).

5.2 The capillary regime: $V_e \gg V_c > V_e^*$

When the rate of evaporation is much larger than the critical capillary velocity the liquid does not have time to flow and replace the evaporated liquid even along the liquid-limit of minimum average curvature. A dry region would

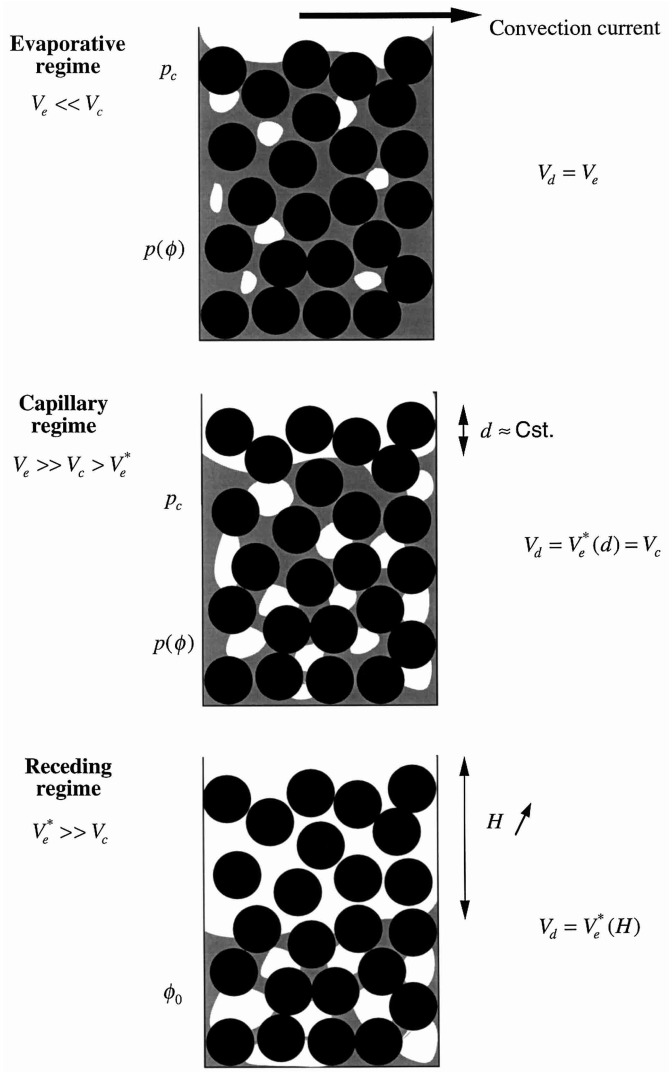

Fig. 3. Scheme of principles of the liquid distribution within the granular packing in the three successive drying regimes (*cf.* text).

thus tend to develop towards the interior of the sample. However the new rate of evaporation (V_e^*) from the new liquid-limit now decreases as it advances and eventually becomes equal to V_c at a distance d, in general much smaller than H_0, from the free surface. At this stage the liquid-limit almost stabilizes. Afterwards the liquid-limit slightly and slowly moves because of the decrease of V_c as ϕ decreases within the wet region, so that d only slightly varies during this capillary period. In conclusion, in this regime the drying rate remains governed by the critical capillary velocity $V_c(\bar{\phi})$ and the liquid-limit remains at a short distance from the free surface (*cf.* Fig. 3).

5.3 The receding regime: $V_e^* \gg V_c$

This regime is reached when the rate of evaporation from the interior of the sample remains larger than the rate of capillary re-equilibration even when the dry front advances towards the interior. In that case the liquid does not move but simply evaporates as soon as the dry front reaches it and there is a receding dry front which finally advances towards the interior of the sample (*cf.* Fig. 3). In this regime the rate of drying is given by V_e^*, which decreases with H, the length of the dry region. If the mean saturation is equal to ϕ_0 in the wet region when this regime starts we deduce from (10) the drying rate expression as a function of $\bar{\phi}$:

$$V_d = \frac{fK}{H_0} \frac{\phi_0}{\phi_0 - \bar{\phi}} \tag{17}$$

where H_0 is the sample length.

5.4 Synthesis

The above expressions equated to (6) can be integrated to obtain the drying rate as a function of time. Around the transition between these asymptotic regimes some significant gradients of ϕ may develop which should be taken into account when estimating the drying rate. We shall nevertheless assume that the transitions are sufficiently abrupt for the dominant phenomenon to suddenly switch over at the expected critical value of ϕ, *i.e.* we assume that three regimes respectively take place for $V_e < V_c$, $V_e > V_c > V_e^*$ and $V_e^* > V_c$. The possible evolutions of V_d as a function of capillary and evaporation velocities can thus be drawn on a single diagram (*cf.* Fig. 4). The schematic aspect of the corresponding concentration profiles at the different stages of drying can be drawn (*cf.* Fig. 5) and, from a qualitative point of view, appear in reasonable agreement with those reported in literature [16] so far as granular packings are concerned.

6 Experiments

6.1 Experimental procedure

We carried out experiments of drying of bead packings filled with ethanol. Four ranges of bead diameters were used which were centered within 15% around a mean value of either 4.5, 17, 34 or 116 μm. Pure ethanol ($\rho = 785$ kg m^{-3}, $\mu = 1.2 \times 10^{-3}$ Pa s, $\sigma = 0.023$ Pa m) was mixed in a container with a certain amount of beads until obtaining a saturated viscous paste. Then this paste was poured in a cylindrical vessel (diameter: 2 cm; depth: 1.5 cm), possibly vibrating the container when it was too viscous, until filling the vessel. The latter was left for settling for a varying time (depending on initial concentration and particle radius) then it was vibrated during 2 min in order to approach the maximum, volumic, solid fraction of a disordered packing. The solid fraction reached after this procedure was 63.5%$\pm$1% except for the smallest particles (4.5 μm) for which it was 50% probably because of some residual, colloidal effects at short distances. A short time after the preparation, as soon as the liquid-air interface at the top of the sample almost reached the first

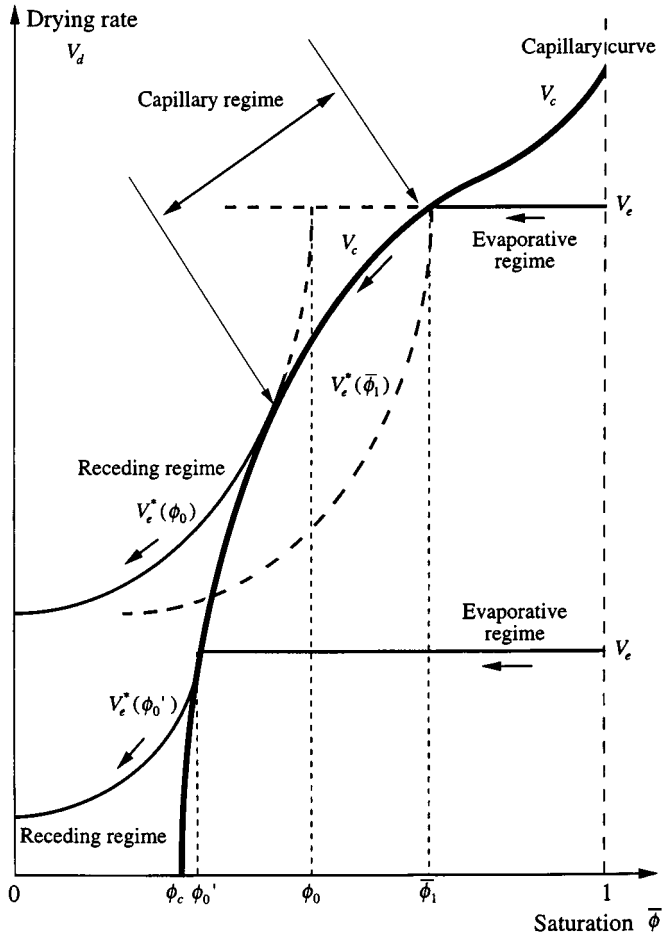

Fig. 4. Conceptual diagram of drying regimes and corresponding evolutions of V_d as a function of $\bar{\phi}$. The evolution of V_d depends on the relative values of the characteristic rates of evaporation and capillary flows. In theory our approach is strictly valid only for asymptotic cases (see text). In practice, around the transition between these asymptotic regimes some significant gradient of ϕ may develop which should be taken into account when estimating the drying rate. We nevertheless assume that the transitions are sufficiently abrupt for the dominant phenomenon to suddenly switch over at the expected critical value of $\bar{\phi}$. The transition from the capillary regime to the receding regime occurs from a point where the V_e^* curve starting from V_e at a saturation ϕ_0 such that it intersects the V_c curve in this point is in fact tangential to this capillary curve. The value of the distance between the liquid-limit and the free surface at a given point (corresponding to a mean saturation $\bar{\phi}_1$) during the capillary regime can be determined from the value of the saturation ϕ_0 at which the V_e^* curve intersecting the capillary curve in this point starts. Indeed in that case we have $d = H_0(1 - \bar{\phi}_1/\phi_0)$. When the level of the drying curve in the CR period is not sufficiently high it meets the capillary curve in a region where the latter rapidly decreases (because it tends towards zero when the saturation tends to the critical saturation). In that case the first V_e^* curve starting at this point remains larger than the V_c curve so that a receding regime directly develops without any period of capillary regime.

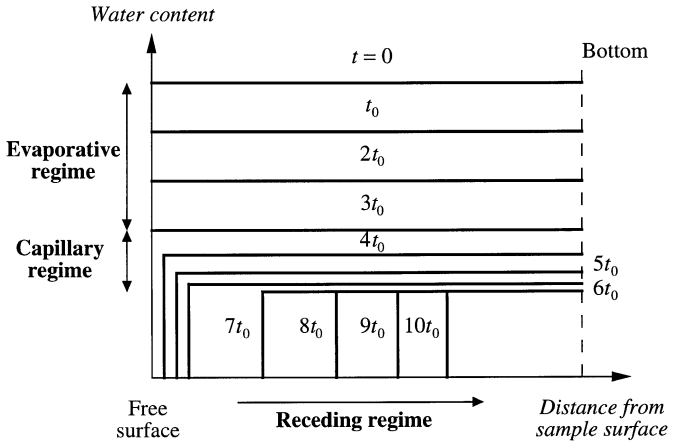

Fig. 5. Schematic representation of the liquid distribution at different stages (time unit t_0) during the drying of a granular packing. In the first (evaporative) regime the density profile is linear and horizontal and advances at an almost constant rate. In the second regime a slight decrease in density appears close to the free surface of the sample and the profile advances at a lower rate. In the last (receding) regime only the part of the profile corresponding to a zero density (close to the free surface) now increases.

bead layer, the vessel was set up on scales and the free surface of the sample submitted to an air current at a given velocity. Four different velocities (ν_i with $i \in [1,4]$) (not measured precisely) were obtained from a fan positioned at different distances or even switched off. The ambient temperature was maintained at 23 °C. The sample weight was recorded with a computer at different time intervals (from 1 to 5 min. depending on material and current velocity).

A typical result (sample weight *vs.* time) is shown in Figure 6. This type of curve does not give precise information concerning the evolution of drying rate with time. The data were first treated in order to obtain the saturation as a function of time. At this stage the drying rate can be obtained by computing the time-derivative of the saturation. In this aim we divided the saturation difference between two instants by the corresponding, elapsed time. In order to limitate the perturbations on velocity resulting from weight fluctuations (due to air current) or possibly from some counterflows effects (*cf.* Sect. 5.1), we used only time intervals corresponding to a saturation difference of 0.1. A mean curve was then fitted manually through the corresponding data and a set of representative points was determined. The uncertainty on the results as presented here is about 25%. The reproducibility of the results presented here within the experimental uncertainty was proved by repeating the tests.

6.2 Results

The results in terms of $\mathrm{d}\bar{\phi}/\mathrm{d}t$ *vs.* $\bar{\phi}$ corresponding to the maximum velocity (ν_1) are presented in Figure 7. In opposition with all existing data we used a representation in

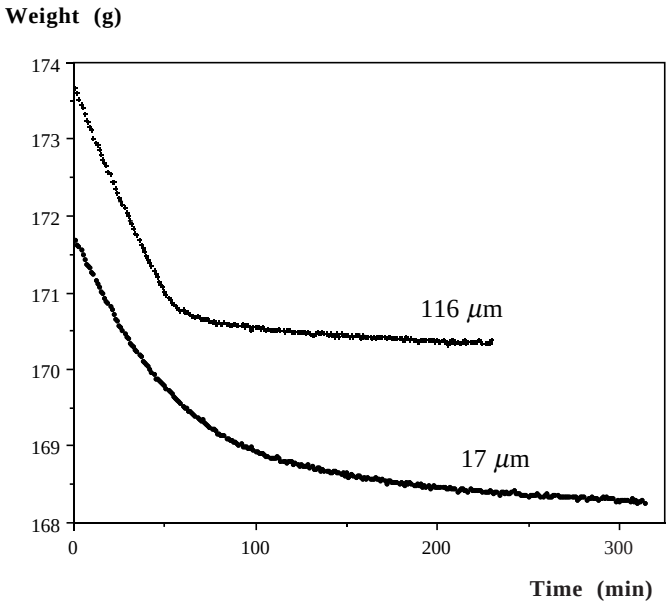

Fig. 6. Drying of bead packings filled with pure ethanol: weight evolution of two samples as a function of time (current velocity: ν_1).

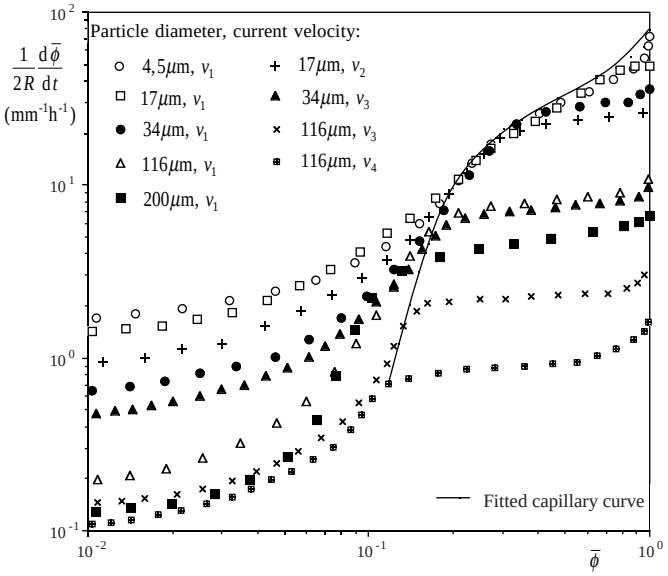

Fig. 8. Drying of bead packings filled with ethanol: drying rate to particle diameter ratio as a function of saturation for the different samples and different current velocities.

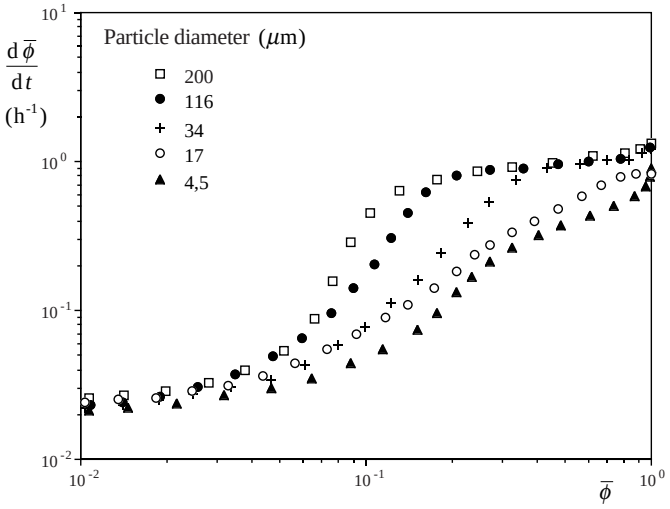

Fig. 7. Drying curves of packings of beads of different diameters (current velocity: ν_1) filled with ethanol.

logarithmic scale in order to observe more clearly the ultimate stages of drying. These data along with other data corresponding to the three smaller current velocities are plot in a diagram $(1/2R)(\mathrm{d}\bar{\phi}/\mathrm{d}t)$ *vs.* $\bar{\phi}$ in Figure 8.

7 Comparison with theory

In these experiments gravity effects remained negligible. Indeed for the largest particles we have $\rho g R H_0/\alpha = 1/10$. From Figure 7 we can see that the current velocity governs the initial evaporation rate within the uncertainty of the measurements. However the evaporation rate keeps this level a larger time for larger particles. The situation is critical for the smallest particles for which the evaporation rate decreases immediately after the beginning of the test. During this first period, which clearly corresponds to the CR period as described in literature, the drying rate is in fact not exactly constant but slowly decreases, as already remarked by Van Brakel [12]. It is remarkable that during this period the drying rate does not depend on particle radius: as predicted by the theory this means that the drying rate is not governed by the liquid flow in the porous medium.

From Figure 7 it also appears that the drying rate in the ultimate stage of drying does not depend on particle radius and tends towards an asymptotic value. This is in agreement with the theory corresponding to the receding regime which predicts that the drying rate simply decreases with the distance of the liquid-limit from the free surface of the sample independently of particle radius and tends towards fK/H_0.

At last in the drying curves of Figure 7 there is an intermediate period during which the drying rate decreases and is all the lower for smaller particle radius. This indicates that this period should more or less correspond to the capillary regime. The validity of this suggestion appears even more clearly when the drying rate is divided by the particle diameter. In that case the theory predicts that the initial and final values of $(1/2R)(\mathrm{d}\bar{\phi}/\mathrm{d}t)$ respectively in the evaporative and receding regimes depend on particle diameter and current velocity, but its intermediate value in the capillary regime should not depend on these parameters. This is exactly what appears in Figure 8. After the (almost) constant rate period, if their initial level is sufficiently high, the curves seem to meet a decreasing master (capillary) curve which they then follow. As the saturation

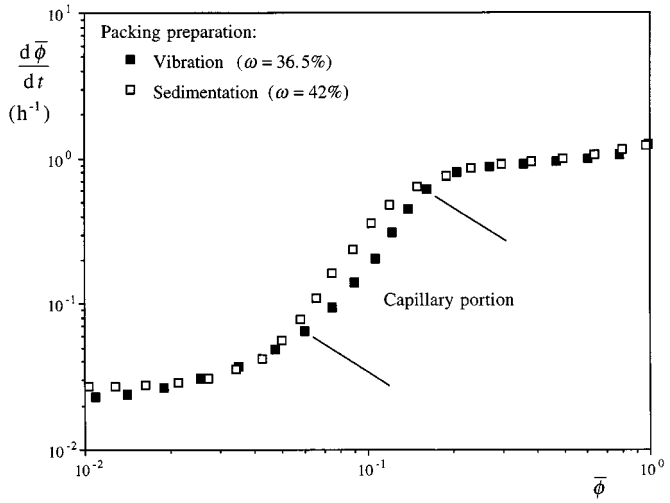

Fig. 9. Drying curve of an ethanol-filled bead packing (diameter: 116 μm, current velocity: ν_1) for two different initial porosities.

decreases they eventually leave this capillary curve and follow a curve which is tangential to it and tends to the final rate of drying. The second stage obviously corresponds to the capillary regime while the third stage is the receding regime. The shape of the curves in the receding regime is very close to that predicted by the theory but considering the rough approximations made in this theory we cannot expect a perfect agreement. When the initial level of the CR period is not high enough the drying curve does not follow the capillary curve when it meets it but simply slowly decreases towards the asymptotic value. This corresponds to the second theoretical situation as represented in Figure 4 for which the receding regime directly follows the evaporative regime because $V_c < V_e^*$.

Note that in Figure 8 the curve corresponding to the smallest particle diameter was in fact slightly higher in the diagram. Its seemed reasonable to associate this effect with the difference in solid fraction between this sample and those made with larger particles. In order to test this idea we compared the results obtained with two different preparations with the same particle type (sedimentation then vibration during five minutes, and sedimentation only) leading to two different solid fractions (*cf.* Fig. 9). The two corresponding drying curves are identical (within the experimental uncertainty) in the initial and last periods but clearly differ in the intermediate period. Following our theoretical analysis this period likely corresponds to the capillary regime during which the drying rate is governed by liquid flow through the solid network. This result in fact appears as a confirmation of the theory since for a given capillary pressure the liquid velocity is more or less proportional to the square of the pore size. On the basis of these results and since it is hard to associate a pore size value to a given solid fraction, in Figure 8 we have simply translated the real curve (4.5 μm, ν_1) of such an amount that it could be superimposed onto the other curves over a wide range of saturation (corresponding to the capillary regime). This translation in fact consists in considering that the effective mean diameter of these beads was 12.5 μm.

8 Conclusion

A quantitative comparison of the theory with existing data cannot be carried out because of the small number of complete drying curves. However this scaling approach already makes it possible to predict and understand the physical origins of the currently observed stages of drying and the corresponding rates of drying. In particular we clearly showed that the FDR period results from a balance between evaporation and capillary liquid flow through a partially desaturated material and is governed by the latter effect. Moreover the CR period is all the shorter for smaller particles and higher intensity of surface convection, and the form of the drying rate curves in the capillary regime is close to that predicted in the three regimes. We suggest that, with some refinements, our approach can be extended to any type of porous materials. This would in particular make it possible to roughly predict the drying rate evolutions without numerical model. In this aim it would be sufficient to determine the "capillary curve" of the material. Thus this might constitute a more successful approach than the "characteristic drying curve" approach [23]. However more experiments and theory are needed in order to take into account gravity effects, to understand the effects of wetting and to describe more precisely the evolution of the saturation distribution within the material.

References

1. J.P. Nadeau, J.R. Puiggali, *Drying - From physical to industrial processes* (Tec&Doc Lavoisier, Paris, 1995) (in French).
2. J.R. Philip, D.A. de Vries, Trans. Am. Geophys. Union **38**, 222-232 (1957).
3. S. Whitaker, W.T.H. Chou, Drying Technol. **1**, 3-33 (1983).
4. T.M. Shaw, Phys. Rev. Lett. **59**, 1671-1674 (1987).
5. N. Ceaglske, O.A. Hougen, Trans. Am. Inst. Chem. Eng. **33**, 283-314 (1937).
6. M. Prat, Drying Technology **9**, 1181-1208 (1991).
7. J. van Brakel, P.M. Heertjes, in *Proc. First Int. Symp. Drying*, edited by A.S. Mujumdar (Science Press, Princeton, 1978), pp. 70-75.
8. P. Chen, D.C.T. Pei, Int. J. Heat Mass Transfer **32**, 297-310 (1989).
9. M. Kaviany, M. Mittal, Int. J. Heat Mass Transfer **30**, 1407-1418 (1987).
10. S. Bories, Proc. Sixth Int. Drying Symp., KL47-KL61 (1988).
11. D.A. de Vries, Int. J. Heat Mass Transfer **30**, 1343-1350 (1987).
12. J. Van Brakel, Adv. Drying **1**, 217-267 (1980).
13. M. Prat, Int. J. Multiphase Flow **19**, 691-704 (1993).
14. M. Prat, Int. J. Multiphase Flow **21**, 875-892 (1995).

15. I.N. Tsimpanogiannis *et al.*, Phys. Rev. E **59**, 4353-4365 (1999).
16. L. Pel, Ph.D. thesis, Eindhoven Techn. Univ., Eindhoven (1995).
17. M. Suzuki, S. Maeda, J. Chem. Eng. Jpn **1**, 26-31 (1968).
18. E.U. Schlünder, Chem. Eng. Sci. **43**, 2685-2688 (1988).
19. K. Hisatake, S. Tanaka, Y. Aizawa, J. Appl. Phys. **73**, 7395-7401 (1993).
20. B.P. Hills *et al.*, Magn. Reson. Imaging **12**, 1053-1063 (1994).
21. P. Coussot *et al.*, C.R. Acad. Sci. (Paris) **327**, 1101-1106 (1999) (in French).
22. I. Chatzis, Ph. D. Thesis, Univ. Waterloo, Canada, 1980.
23. C. Moyne, C. Basilico, J.C. Batsale, A. Degiovanni, in *Modelling and applications of transport phenomena in-porous media*, Ch. 5, edited by J. Bear, J.M. Buchlin (Kluwer Acad. Publ., London, 1991).